Particle & Particle Systems Characterization
www.particle-journal.com

Synthesis and Characterization of Pressure and Temperature Dual-Responsive Polystyrene Microbeads

*Cun Zhu, Rui Deng, Jie Zeng, Gamal E. Khalil, Dana Dabiri, Zhongze Gu, and Younan Xia**

A facile approach to the synthesis of pressure and temperature dual-responsive polystyrene (PS) microbeads with controlled sizes via dispersion polymerization is described. Three different luminophors are selected and directly introduced into the reaction system and thus incorporated into the resultant PS microbeads during polymerization. By manipulating the reaction conditions, including concentrations of the initiator and monomer, polarity of the reaction medium, and injection rate for the monomer, uniform PS microbeads with sizes ranging from 1 to 5 μm are obtained. When a light source centered at 365 nm is used to excite all the luminophors in the PS beads, three distinct and resolvable emission peaks corresponding well with the luminophors are observed. By taking advantage of their sensitive responses to both pressure and temperature, the PS beads can be utilized for quantitative measurements of these two stimulations simultaneously. The PS beads loaded with multiple luminophors have the ability to serve as building blocks for the fabrication of novel sensing and imaging devices and therefore provide a promising strategy for the study of aerodynamics.

1. Introduction

In recent years, functional colloidal particles have drawn considerable interest owing to their remarkable physicochemical properties. Thanks to their controllable size, large specific surface area, and easy dispersion/manipulation, colloidal particles have been widely used as templates or hosts for the loading of functional molecules, quantum dots, and/or metal nanocrystals.[1–9] In particular, colloidal particles encapsulated with organic luminophors have emerged as a class of promising and highly sensitive indictors for the purpose of sensing and imaging.[10–16] During the last decade, tremendous efforts have been devoted to the study of this class of colloidal particles, resulting in the development of many protocols for the fabrication of colloidal particles loaded with various types of luminophors.[17–21]

In general, two major strategies have been developed for the preparation of luminophor-loaded colloidal particles, i) incorporation of the luminophors during the formation of colloidal particles via covalent or noncovalent binding of the luminophor molecules with polymer chains and ii) adsorption or entrapment of the luminophors in the polymer matrix of pre-formed colloidal particles via swollen, or through coupling with the surface-reactive functional groups.[22] Each approach has its own advantages and limitations. For the first approach, the introduction of luminophors into the reaction system might bring disturbance to the formation of colloidal particles, leading to a broad distribution in size for the resultant particles. For the second approach, despite its little influence on the size distribution of pre-formed colloidal particles, it is not easy to obtain homogeneous loading of a luminophor inside the colloidal particles. The enrichment of luminophors in some regions of the particles might result in quenching of the luminescence and thus loss in luminescence intensity. Furthermore, most syntheses focused on the fabrication of colloidal particles loaded with only one or two luminophors,[23–27] and only a few of them had ever addressed the capability to load multiple luminophors. In addition to the obvious technical challenges in finding a common solvent and polymer system to accommodate multiple luminophors, the resultant particles may also suffer from issues such as energy transfer among the luminophors and thus quenching of luminescence.[28] Therefore, it is still a challenge to develop a facile method for generating multiple-responsive colloidal particles with uniform size and resolvable emission peaks for sensing and imaging applications.

Herein, we report a facile route to the synthesis of pressure and temperature dual-responsive polystyrene (PS) microbeads using the dispersion polymerization method. Three luminophors that could serve as the pressure indicator, temperature indicator, and a reference, respectively, were directly introduced

C. Zhu, Dr. R. Deng, Prof. J. Zeng, Prof. Y. Xia
The Wallace H. Coulter Department of Biomedical Engineering, School of Chemistry & Biochemistry and School of Chemical & Biomolecular Engineering
Georgia Institute of Technology
Atlanta, GA, 30332, USA
E-mail: younan.xia@bme.gatech.edu
C. Zhu, Prof. Z. Gu
State Key Laboratory of Bioelectronics
School of Chemistry and Chemical Engineering
Southeast University
Nanjing, 210096, P. R. China
Prof. G. E. Khalil, Prof. D. Dabiri
Department of Aeronautics and Astronautics
University of Washington
Seattle, WA 98195, USA

DOI: 10.1002/ppsc.201300024

into the reaction system and incorporated into the PS microbeads during polymerization. We also systematically investigated the influence of various reaction conditions, including the concentrations of both initiator and monomer, the polarity of reaction medium, and the injection rate for monomer, on the size and size distribution of the microbeads. By adjusting these reaction parameters, the microbeads could be readily prepared with sizes controlled in the range of 1 to 5 μm. The PS microbeads loaded with three luminophors exhibited excellent optical properties, with strong responses to both pressure and temperature. When they were excited with a light source centered at 365 nm, three separate and distinct emission peaks corresponding to the introduced luminophors were observed. By varying either pressure or temperature applied to the microbeads, apparent changes were observed for the fluorescence peak intensity corresponding to the respective luminophors, while that of the reference luminophor was essentially unchanged during the entire measurement. As such, the PS microbeads loaded with multiple luminophors are well-suited for quantitatively monitoring the state of applied airflow including both pressure and temperature. We believe this work will provide a promising strategy for the design and fabrication of novel optical devices for remote sensing and imaging applications.

2. Experimental Section

2.1. Chemicals and Materials

Poly(vinyl pyrrolidone) of 55 000 in molecular weight (PVP55), 2,2'-azobis(2-methylpropionitrile) (AIBN), styrene (St), and ethanol were all purchased from Sigma-Aldrich. Pt(II) octaethylporphine (Dye A) and Eu(III) thenoyltrifluoroacetonate (Dye B) were obtained from Frontier Scientific and Gelest, respectively. Coumarin 6 (Dye C) was purchased from Luminescence Technology Corporation. Deionized water with a resistivity of 18.2 MΩ cm was used for all the syntheses. All chemicals were used as received.

2.2. Synthesis of Microbeads with Controlled Sizes and Loaded with Three Luminophors

In a typical synthesis, 130 mg of PVP55, 15 mL of ethanol, 2 mg of Dye A, 30 mg of Dye B, 1 mg of Dye C, and H_2O at a specific volume were placed in a 50 mL flask. The solution was preheated to 80 °C in air under magnetic stirring. Meanwhile, a specific amount of AIBN was dissolved in styrene at room temperature, and then introduced into the flask at a specific rate using a pipette or syringe pump. The polymerization was allowed to proceed at 80 °C for 24 h. The resultant PS microbeads were collected by centrifugation and washed with water three times. **Table 1** shows the detailed experimental conditions, including the amounts of H_2O, AIBN, and the injection rate for styrene monomer associated with each synthesis.

2.3. Instrumentation

Scanning electron microscopy (SEM) images were taken using a field-emission scanning electron microscope (Nova NanoSEM 230, Hillsboro, OR) operated at an accelerating voltage of 5 kV. The optical microscopy images of the PS beads were taken using a confocal laser scanning microscope (Carl Zeiss, Thornwood, NY). The pressure and temperature responsiveness of the PS beads were measured using a dynamic flow system (the PMT survey apparatus) described in a prior publication.[29] A mercury short arc lamp equipped with a band pass filter centered at 365 nm was used to excite the luminophors in these beads.

3. Results and Discussion

3.1. Selection of Luminophors

In a fluorescent system containing multiple luminophors, there is often a risk of luminescence quenching due to the interactions between different luminophors, including the quenching caused by energy transfer between different luminophors and the self-quenching through short-range interactions.[30] When the absorption peak of one luminophor overlaps with the emission peak of another luminophor, energy will be spontaneously transferred within the overlapped region, leading to fluorescence depolarization and quenching. On the other hand, a relatively high local density of luminophors can make the luminophor molecules interact strongly or physically contact with each other, resulting in self-quenching of their luminescence and decrease of the overall fluorescence quantum yield. It is not difficult to realize that self-quenching of the luminescence strongly depends on the distance between adjacent luminophor molecules. By optimizing the concentrations of luminophors, self-quenching could be effectively mitigated. Moreover, the

Table 1. Reaction conditions for the synthesis of PS microbeads with different sizes and loaded with three different luminophors.

Monomer St [mL]	AIBN [mg]	PVP [mg]	Ethanol [mL]	H2O [mL]	RSta) [mL/h]	T [°C]	Diameter [μm]
1.67	18	130	15	1.67	one-shot	80	1.1 (Figure 2A)
1.67	33	130	15	1.67	one-shot	80	1.7 (Figure 2B)
3.75	18	130	15	0	3.75	80	3.6 (Figure 2C)
3.75	18	130	15	0	2	80	4.9 (Figure 2D)

a)The injection rate for monomer styrene.

Part. Part. Syst. Charact. 2013,
DOI: 10.1002/ppsc.201300024

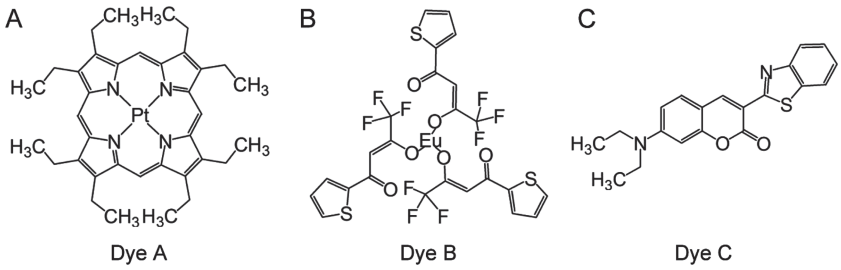

Figure 1. Structures of luminophors that were used for the synthesis of pressure and temperature dual-responsive PS microbeads: A) pressure and temperature sensitive luminophor Pt(II) octaethylporphine, B) temperature sensitive luminophor Eu(III) thenoyltrifluoroacetonate, and C) reference luminophor Coumarin 6.

fluorescence quantum yield of a luminophor usually depends on the wavelength of the excitation light; the maximum yield can be achieved when the wavelength of the excitation light matches that of the absorption peak of the luminophor. To obtain emission spectrum with resolvable peaks for all luminophors and with optimized intensities, it is important to carefully select proper luminophors by considering both their optical properties and loading concentrations.

We chose three different luminophors from a variety of conceivable candidates as functional components for the construction of a pressure and temperature dual-responsive system: Pt(II) octaethylporphine (Dye A) for monitoring pressure change, Eu(III) thenoyltrifluoroacetonate (Dye B) for temperature change, and Coumarin 6 (Dye C) as a reference dye. The structures of these luminophors are shown in **Figure 1**. Uniform PS microbeads were used as a matrix to host these luminophors, which could also serve as building blocks for the construction of sensing and imaging devices. Since these luminophors could easily interact with the hydrophobic polymer chains via noncovalent binding and adsorption, they were directly mixed with monomer styrene and then embedded in the polymer matrix during polymerization. Figure S1 in the Supporting Information shows the emission spectra recorded from PS microbeads loaded with three luminophors, which were synthesized using the same protocol but with different loading amounts for the luminophors. By optimizing the concentrations of the luminophors used for the synthesis, the resultant PS beads could be adjusted to exhibit resolvable emission spectra with three distinct and separate peaks located at 650, 615, 510 nm, respectively (Supporting Information Figure S1C).

3.2. Size Control of the Luminescent PS Microbeads

The PS microbeads could be loaded with three different luminophors and still be prepared with uniform, controllable sizes via dispersion polymerization. The final size and size distribution of the resultant PS beads depended on a range of reaction conditions, including the reaction temperature, the polarity of reaction medium, the concentrations of initiator and monomer, and the stabilizer. To achieve the synthesis in a controllable fashion and thus generate PS beads with adjustable sizes, we carefully evaluated these parameters during the polymerization. **Figure 2** shows representative SEM images of the luminescent PS beads with a range of diameters synthesized under different reaction conditions. When the synthesis was conducted with AIBN at an amount of 18 mg, the final product was dominated by PS beads with an average diameter of ca. 1.1 μm (Figure 2A). When the amount of AIBN was increased to 33 mg, the final size of the resultant PS beads was slightly increased to ca. 1.7 μm (Figure 2B). The PS beads obtained under these two different conditions had very similar narrow size distribution. By increasing the concentration of AIBN, more short polymer chains would be developed from the free radicals and thus existed in the reaction system, leading to a reduction in the number of insoluble long polymer chains. In this case, fewer preliminary particles would be formed and precipitated from the reaction medium, eventually leading to the growth of PS beads with larger sizes.

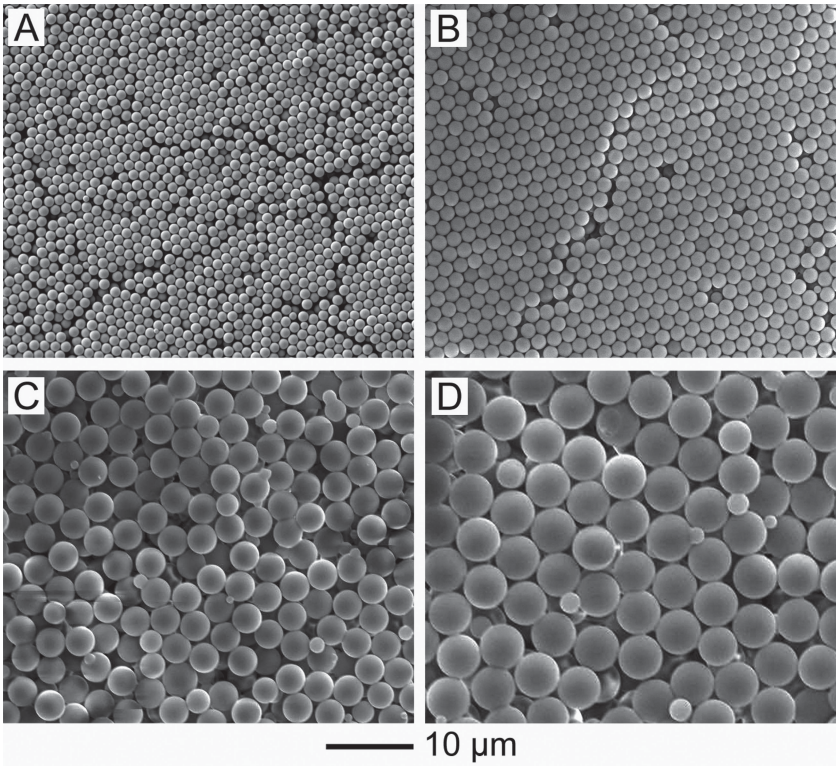

Figure 2. SEM images of PS microbeads with different sizes that had been loaded with three luminophors. The average diameters of the PS microbeads were A) 1.1, B) 1.7, C) 3.6, and D) 4.9 μm.

Besides the concentration of initiator, the polarity of reaction medium, the concentration and injection rate for monomer could also greatly affect the size of resultant PS beads. Reducing the polarity of the reaction medium could effectively increase the solubility of monomer styrene and short polymer chains in the reaction system, resulting in the formation of fewer insoluble preliminary PS particles and thus the generation of PS beads with larger sizes. In addition, increasing the concentration of monomer in the reaction system, or reducing the injection rate for monomer was also beneficial to the generation of PS beads with larger sizes. Since the polarity of H_2O is stronger than ethanol, we conducted the synthesis in the absence of water in an effort to reduce the polarity of reaction medium and further increase the size of resultant PS beads. We also increased the concentration of monomer styrene involved in the polymerization by introducing them into the reaction system at a controlled rate with the help of a syringe pump instead of one-shot injection to further reduce the reaction rate. As a result, we could increase the final size of the PS beads by generating less insoluble long polymer chains at the beginning of the polymerization. When monomer styrene was introduced into the reaction system at a rate of 3.5 mL/h, PS beads with an average diameter of ca. 3.6 μm were obtained (Figure 2C). Reducing the injection rate to 2.0 mL/h led to the formation of PS beads with an average diameter of ca. 4.9 μm (Figure 2D), indicating that PS beads with larger sizes could be obtained at a lower polarity for the reaction medium, a higher concentration but slower injection rate for the monomer. However, PS beads with a somewhat broader distribution in size were obtained under these reaction conditions. We believe that this broadening of size distribution can be mainly attributed to the insufficient formation of insoluble preliminary PS particles as active sites at the initial stage of a synthesis. In this case, the continuous precipitation of preliminary PS particles throughout the synthesis could not be effectively inhibited, leading to a boarder size distribution for the resultant beads.

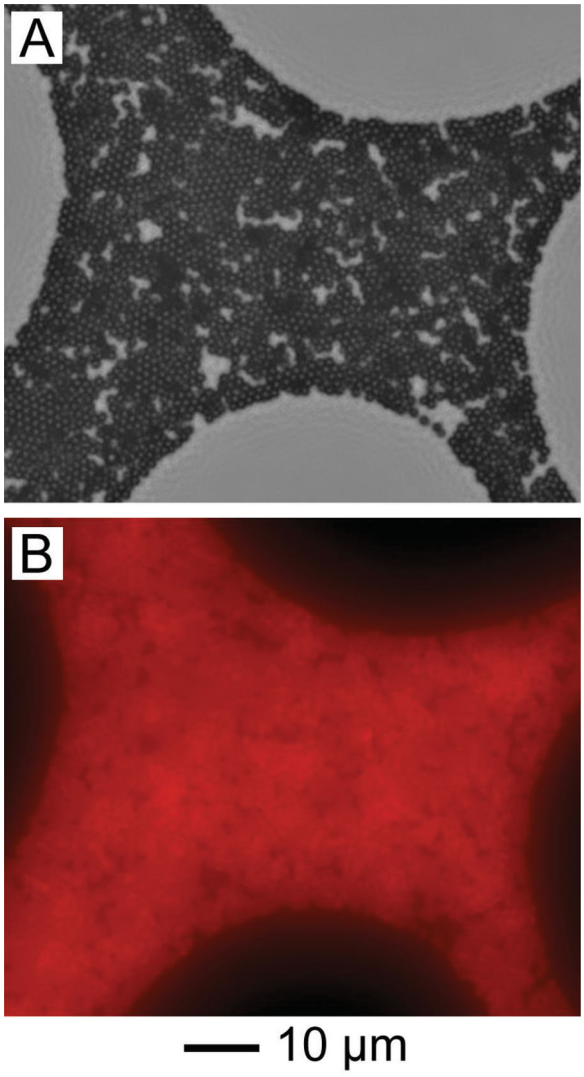

Figure 3. A) Phase contrast optical microscopy image of PS microbeads 1.7 μm in diameter, which had been loaded with three luminophors and B) the corresponding luminescence microscopy image. The samples were excited with a light source peaked at 365 nm, and the exposure time was 200 ms.

3.3. Fluorescence Properties of the PS Microbeads

We utilized a confocal laser scanning microscope to qualitatively evaluate the fluorescence properties of the PS microbeads loaded with three luminophors. In our previous report, we have proven that the size of PS beads loaded with two luminophors had essentially no influence on their fluorescence performance.[23] On the basis of this observation, we selected luminescent PS beads with a size of 1.7 μm for the study of their optical properties because they had very narrow size distribution, which would be beneficial to the assembly of these beads into a monolayer array on a solid substrate. **Figure 3** shows the phase contrast microscopy image and the corresponding luminescence microscopy image. In a typical process, an aqueous suspension of the PS microbeads was applied to the surface of a glass substrate. During the drying process, the PS beads self-assembled into a hexagonal array over a relatively large area (Figure 3A). Figure 3B shows the corresponding luminescence microscopy image of these beads when excited with a light source centered at 365 nm. The exposure time was set to 200 ms. The strong and homogeneous luminescence emitted from these PS beads indicated that the luminophors had been successfully loaded into the polymer matrix with a high loading efficiency. As a result, it was quite difficult to distinguish an individual PS bead from the adjacent beads from the luminescence microscopy image. Moreover, these PS beads exhibited red color when excited with the light source, indicating that both Dye A and Dye B made contributions to the fluorescence, which was desired for the subsequent pressure and temperature measurements.

3.4. Pressure Responsiveness of the Luminescent PS Microbeads

To investigate the pressure responsiveness of the PS microbeads doped with three luminophors, we used a dynamic flow

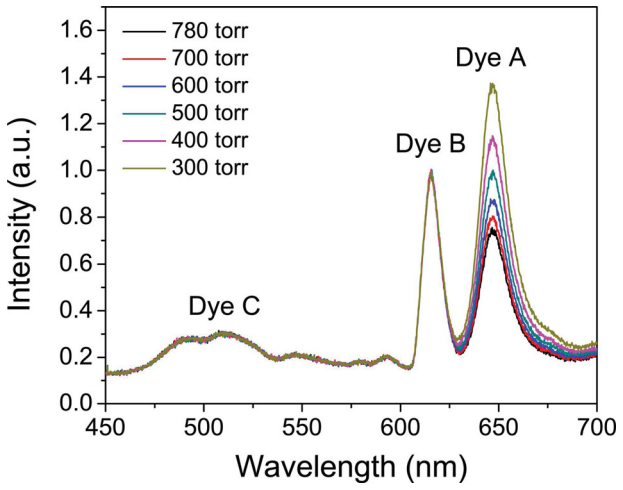

Figure 4. Emission spectra recorded from the three luminophors loaded in PS microbeads of 1.7 μm in diameter as a function of pressure. The samples were excited with a light source peaked at 365 nm.

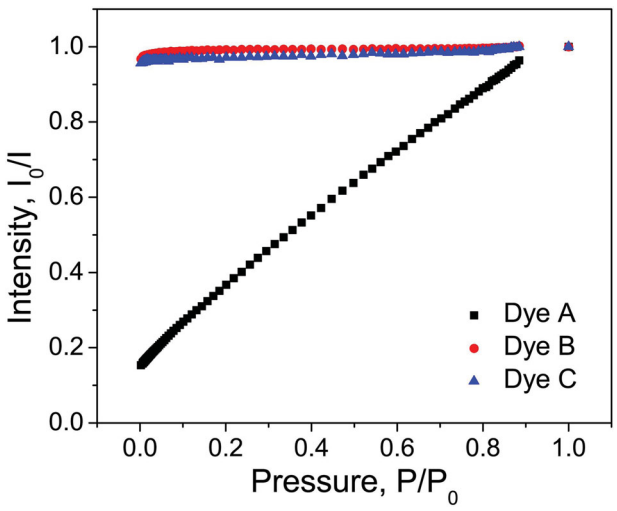

Figure 5. Stern–Volmer pressure plots for the PS microbeads loaded with three luminophors as a function of pressure. The samples were excited with a light source peaked at 365 nm.

system to monitor their fluorescence spectra by introducing airflow with a controlled pressure into the chamber. The PS beads were excited with a light source centered at 365 nm. **Figure 4** shows the emission spectra recorded from these PS microbeads in response to the change of pressure. The emission peaks of all luminophors could be easily resolved, while the change in the fluorescence intensity clearly revealed their responsiveness to the pressure. By normalizing the fluorescence spectra collected under various pressures to that of Dye B obtained at 780 torr, it can be seen that only the emission peak of Dye A exhibited significant change in fluorescence intensity when the pressure was varied. The peak intensity constantly increased when the pressure of the airflow was decreased from 780 torr to 300 torr. In comparison, the peaks of Dyes B and C were essentially the same during this process. These results implied that the fluorescence intensity of Dye A was inversely proportional to the pressure, while those of Dyes B and C were insensitive to the change of pressure. This observation was consistent with the results obtained from PS beads loaded with two luminophors only, which were synthesized using the same protocol but in the absence of Dye B (Supporting Information, Figure S2).

Since the luminescence of Dye A could be effectively quenched by oxygen, increasing the concentration of oxygen in the chamber by increasing the pressure would greatly increase the opportunity for oxygen molecules to interact with the luminophors loaded in the PS beads and thus lead to stronger quenching of the luminescence and thus reduction in its intensity. In this case, the fluorescence intensity of Dye A depended on the concentration of oxygen in the system. The luminescence quenching by oxygen could be quantitatively calculated using the modified Stern–Volmer equation[23,31–33]:

$$\frac{I_0}{I} = \frac{k_n + k_d + k_q[O_2]}{k_n + k_d + k_q[O_2]_0} = \frac{(k_n + k_d)}{k_n + k_d + k_q[O_2]_0} + \frac{k_q[O_2]_0}{k_n + k_d + k_q[O_2]_0}\left(\frac{[O_2]}{[O_2]_0}\right) \quad (1)$$

where I_0 and I refer to the fluorescence intensity in the presence of oxygen at reference and specific concentrations, respectively; k_n and k_d refer to the natural radiative decay rate constant, and the radiationless decay rate constant, respectively; k_q represents the quenching rate constant by oxygen, which describes the efficiency of the collision and interaction between the oxygen and luminophor; τ is the emission lifetime, and $[O_2]$ is the concentration of oxygen. It is not difficult to find that there is a linear relation between the I_0/I and $[O_2]/[O_2]_0$, where the fluorescence intensity of the luminophor was inversely proportional to the concentration of oxygen and thus the pressure. Since in the airflow the ratio of $[O_2]/[O_2]_0$ equaled to that of P/P_0, a linear relation could be deduced from the plot of I_0/I versus P/P_0. **Figure 5** shows the Stern–Volmer plots for the PS microbeads loaded with three luminophors in response to the change of pressure. From the Stern-Volmer plot of Dye A, its intercept and slope were estimated to be 0.165 and 0.886, respectively. In this case, the relationship between I_0/I and P/P_0 could be described as:

$$\frac{I_0}{I} = 0.165 + 0.886\frac{P}{P_0} \quad (2)$$

In this case, it is convenient to quantitatively calculate the estimate value of the fluorescence intensity (I) of Dye A or the pressure (P) of airflow once we know one of them.

3.5. Temperature Responsiveness of the Luminescent PS Microbeads

We also studied the temperature responsiveness of the PS microbeads loaded with three luminophors by monitoring their fluorescence spectra while varying the applied temperature. The sensing array composed of the luminescent PS beads was heated from 10 °C to 50 °C by a heater. The emission spectra from the PS beads collected at different temperatures were

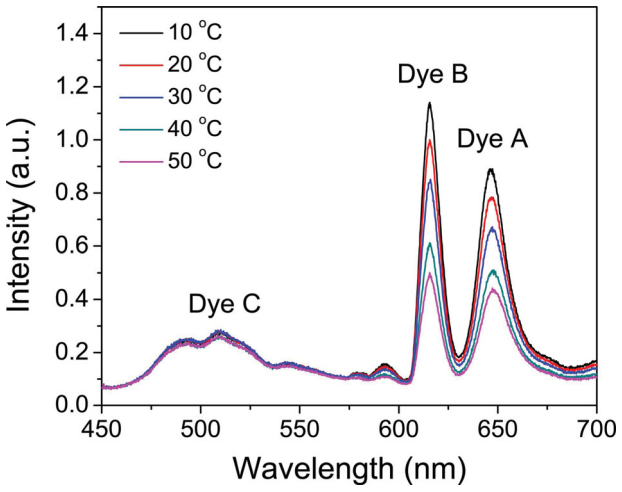

Figure 6. Emission spectra recorded from the three luminophors loaded in PS microbeads of 1.7 µm in diameter as a function of temperature. The samples were excited with a light source peaked at 365 nm.

normalized to that of Dye B obtained at 20 °C. As shown in **Figure 6**, it was found that the fluorescence intensity of both Dye A and Dye B dropped along with the elevation of temperature. When the temperature reached 50 °C, the fluorescence intensities of both Dye A and Dye B became only about half of those obtained at 10 °C. The fluorescence intensities of both Dyes A and B were inversely proportional to the temperature. In comparison, no apparent change was observed for the emission peak of the reference Dye C during the entire measurement, indicating that Dye C was sensitive to neither pressure nor temperature. This conclusion was also validated by the results from PS microbeads loaded with two luminophors only, which were synthesized using the same protocol but in the absence of Dye A (Supporting Information Figure S3).

We believe that the temperature responsiveness of Dyes A and B can be attributed to different mechanisms. For Dye A, its temperature responsiveness is likely associated with the difference in rate for oxygen to diffuse into the polymer matrix at different temperatures. A higher temperature would accelerate the Brownian motion of oxygen molecules, leading to a quicker diffusion of oxygen into the polymer matrix to interact with the luminophor loaded in the PS beads, eventually resulting in more effective dynamic oxygen quenching of its luminescence. For Dye B, a luminophor insensitive to oxygen, its strongest emission at approximately 615 nm originates from the $^5D_0$ energy level of Eu^{3+} ion through the $^5D_0$ to $^7F_2$ transition.[34,35] In this case, the thermal deactivation of $^5D_0$ and $^5D_1$ europium energy levels, as well as the thermal deactivation of $^5D_1$ to $^5D_0$ level, would result in a nonradiative process and thus contribute to its temperature responsive property.[34–37] Since the temperature responsiveness of Dye A was mainly associated with the dynamic oxygen quenching of its luminescence, we prefer to utilize Dye B as a temperature-sensitive luminophor for monitoring the temperature change. It should be emphasized that the peak positions of all these three luminophors did not exhibit any change during the measurement, and both pressure and temperature responsiveness of the PS microbeads were reversible and repeatable. As such, these luminescent PS microbeads are well-suited as building blocks for the fabrication of novel sensing and imaging devices.

4. Conclusions

In summary, we have demonstrated that PS microbeads could be loaded with three different luminophors and still be synthesized with controllable sizes and narrow size distribution using a method based on dispersion polymerization. We also investigated the effects of various reaction parameters, including, for example, the concentrations of initiator and monomer, the polarity of reaction medium, and the injection rate of monomer, on both the size and size distribution of the resultant PS microbeads. By optimizing the concentrations of all luminophors used for the synthesis, we obtained luminescent PS microbeads with three well-resolved emission peaks for the luminophors. The PS microbeads exhibited good responses to both pressure and temperature. The change in the fluorescence intensity of indicative luminophors could be clearly observed when the pressure or temperature was varied whereas that of the reference luminophor was essentially unchanged. As a result, the PS microbeads could be directly used for quantitative measurements of the state of applied airflow such as the pressure and temperature. In principle, these PS microbeads loaded with multiple luminophors could serve as building blocks for the fabrication of novel sensing and imaging devices sought by a variety of applications.

Supporting Information

Supporting Information is available from the Wiley Online Library or from the author.

Acknowledgement

This work was supported in part by the NSF (IDR-0929864) and startup funds from Georgia Institute of Technology. As a visiting student from Southeast University, C.Z. was also partially supported by a fellowship from the China Scholarship Council.

Received: January 18, 2013
Published online:

[1] Y. Li, E. C. Y. Liu, N. Pickett, P. J. Skabara, S. S. Cummins, S. Ryley, A. J. Sutherlandc, P. O'Brien, *J. Mater. Chem.* **2005**, *15*, 1238.
[2] S. Scarmagnani, Z. Walsh, C. Slater, N. Alhashimy, B. Paull, M. Mack, D. Diamond, *J. Mater. Chem.* **2008**, *18*, 5063.
[3] T. Kawawaki, Y. Takahashi, T. Tatsuma, *Nanoscale* **2011**, *3*, 2865.
[4] C. W. Blackledge, T. Tabarin, E. Masson, R. J. Forster, T. E. Keyes, *J. Nanopart. Res.* **2011**, *13*, 4659.
[5] I. Yosef, D. Avnir, *J. Nanopart. Res.* **2011**, *13*, 3929.
[6] Y.-H. Li, T. Song, J.-Q. Liu, S.-J. Zhu, J. Chang, *J. Mater. Chem.* **2011**, *21*, 12520.
[7] S. Mandal, C. Ghatak, V. G. Rao, S. Ghosh, N. Sarkar, *J. Phys. Chem. C* **2012**, *116*, 5585.

[8] L. Huang, Z. Luo, H. Han, *Chem. Commun.* **2012**, *48*, 6145.
[9] C. W. Kim, U. Pal, S. Park, J. Kim, Y. S. Kang, *Chem. Eur. J.* **2012**, *18*, 12314.
[10] S. Santra, P. Zhang, K. Wang, R. Tapec, W. Tan, *Anal. Chem.* **2001**, *73*, 4988.
[11] L. Wang, C. Yang, W. Tan, Nano Lett. *Nano Lett.* **2005**, *5*, 37.
[12] F. Kimura, G. Khalil, N. Zettsu, Y. Xia, J. Callis, M. Gouterman, L. Dalton, D. Dabiri, M. Rodriguez, *Meas. Sci. Technol.* **2006**, *17*, 1254.
[13] B. J. Melde, B. J. Johnson, P. T. Charles, *Sensors* **2008**, *8*, 5202.
[14] C.-S. Chu, Y.-L. Lo, T.-W. Sung, *Talanta* **2010**, *82*, 1044.
[15] J. E. Lee, N. Lee, H. Kim, J. Kim, S. H. Choi, J. H. Kim, T. Kim, I. C. Song, S. P. Park, W. K. Moon, T. Hyeon, *J. Am. Chem. Soc.* **2010**, *132*, 552.
[16] R. J. Meier, S. Schreml, X. Wang, M. Landthaler, P. Babilas, O. S. Wolfbeis, *Angew. Chem. Int. Ed.* **2011**, *50*, 10893.
[17] N. A. M. Verhaegh, A. van Blaaderen, *Langmuir* **1994**, *10*, 1427.
[18] A. P. R. Johnston, B. J. Battersby, G. A. Lawrie, M. Trau, *Chem. Commun.* **2005**, *0*, 848.
[19] C. R. Miller, R. Vogel, P. P. T. Surawski, K. S. Jack, S. R. Corrie, M. Trau, *Langmuir* **2005**, *21*, 9733.
[20] J.-S. Song, F. Tronc, M. A. Winnik, *Polymer* **2006**, *47*, 817.
[21] X. Zhang, Y. Ren, M. Chen, L. Wu, *J. Colloid Interface Sci.* **2011**, *358*, 347.
[22] M. Bele, O. Siiman, E. Matijevic, *J. Colloid Interface Sci.* **2002**, *254*, 274.
[23] S. H. Ima, G. E. Khalil, J. Callis, B. H. Ahnb, M. Gouterman, Y. Xia, *Talanta* **2005**, *67*, 492.
[24] S. R. Corrie, G. A. Lawrie, M. TrauLangmuir *Langmuir* **2006**, *22*, 2731.
[25] P. J. Cywinskia, A. J. Moroa, S. E. Stancab, C. Biskupb, G. J. Mohra, *Sens. Actuators B* **2009**, *135*, 472.
[26] B. J. Basu, S. Venkatraman, *J. Fluoresc.* **2009**, *19*, 479.
[27] F. Su, R. Alam, Q. Mei, Y. Tian, C. Youngbull, R. H. Johnson, D. R. Meldrum, *PLoS ONE* **2012**, *7*, e33390.
[28] M. I. J. Stich, S. Nagl, O. S. Wolfbeis, U. Henne, M. Schaeferling, *Adv. Funct. Mater.* **2008**, *18*, 1399.
[29] F. Kimura, M. Rodriguez, J. McCann, B. Carlson, D. Dabiri, G. E. Khalil, J. B. Callis, Y. Xia, M. Gouterman, *Rev. Sci. Instrum.* **2008**, *79*, 074102.
[30] M. Montalti, L. Prodi, N. Zaccheroni, A. Zattoni, P. Reschiglian, G. Falini, *Langmuir* **2004**, *20*, 2989.
[31] O. Stern, M. Volmer, *Phys. Z.* **1919**, *20*, 183.
[32] J. Kavandi, J. Callis, M. Gouterman, G. Khalil, D. Wright, E. Green, D. Burns, B. McLachlan, *Rev. Sci. Instrum.* **1990**, *61*, 3340.
[33] J. R. Lakowicz, *Principles of Fluorescence Spectroscopy*, **2nd ed.**, Kluwer Academic/Plenum Press, New York **1999**.
[34] G. E. Khalil, K. Lau, G. D. Phelan, B. Carlson, M. Gouterman, J. B. Callis, L. R. Dalton, *Rev. Sci. Instrum.* **2004**, *75*, 192.
[35] B. B. J. Basu, N. Vasantharajan, *J. Lumin.* **2008**, *128*, 1701.
[36] M. L. Bhaumik, *J. Chem. Phys.* **1964**, *40*, 3711.
[37] K. H. Drexhage, *Dye Lasers*, Springer, Berlin **1973**, Ch. 5.